Journal of Structural Geology, Vol. 8, Nos 3/4, 373 to 387, 1986
Printed in Great Britain

0191-8141/86 $03.00 + 0.00

Deformation and displacement of the Jura cover on its basement

J. L. MUGNIER and P. VIALON

Institut de Recherche Interdisciplinaire de Géologie et de Mécanique (Grenoble), Post Box 68, 38402 St Martin d'Heres Cedex, France

(*Received* 1 *July* 1984; *accepted in revised form* 16 *April* 1985)

Abstract—The sedimentary cover of the Internal Jura, displaced over its basement, conforms well with the model of a thin-skinned thrust sheet. The wedge-shaped sheet, which includes a thick sequence of molasse deposited ahead of the Alpine front, slid over the basement/cover interface. The Alpine crustal thrust sheets created a load at the south-east end of the overthrust European plate. Molasse was deposited on the bent plate, and the internal part of the basin was progressively affected by thrusting.

This process also induced deformation and displacements in the foreland: gravity spreading in the internal molasse, and a forward motion by rigid slipping. Movement led to a horizontal push, causing deformation by indentation in the Internal Jura. In the plateaux of the External Jura, there is very little extension in the cover and minimal shortening in the basement. This shortening induced a décollement under the plateaux. Over the Bresse graben, gravity sliding occurred in the form of huge landslides.

These contrasts in the origin of the Jura structures, along a median cross-section from Thonon to Arbois, are shown by geophysical data, construction of a balanced cross-section and calculations of realistic mechanical models for the bending of the foreland plate and for the motion of the cover sheet.

INTRODUCTION

THE JURA has been the subject of much geological study. The bibliography of Caire (1963), though not exhaustive, nonetheless contains 340 papers, and many important papers have been written since 1963. Numerous drill-hole data (see Appendix 1) and geophysical data provide important constraints on the subsurface structure. However, in spite of this detailed knowledge (or precisely because of it), there is no well-accepted general interpretation for the formation of these mountains. No single geodynamic model adequately incorporates the full set of particular local details. However, no detail can be neglected. Some details are locally important or fortuitous, whereas others are related to the regional events. The facts need to be weighed according to their importance, and we can use quantitative models to attempt to arrange them. At the same time we must be careful not to allow our assessment to be influenced by our hypotheses.

We have used analytical methods to estimate the importance of the following features, generally considered to be important in understanding the orogenesis of the Jura Mountains (Mattauer 1973, Chauve *et al.* 1980, Laubscher 1980).

(1) The Jura lies between two structures on a continental scale: the Alpine collision zone to the south-east, and the Rhine and Bresse grabens to the north and west (Fig. 1). This must be taken into account in order to define the main tectonic events in the Jura; these being extensional events during Oligocene time, and shortening events at the Miocene–Pliocene boundary.

(2) In the frontal parts of the Jura, the borders are either subsiding rifts (Bresse, Rhine graben), elevated zones (Schwarzwald, Vosges, Bas-Dauphiné–Ile

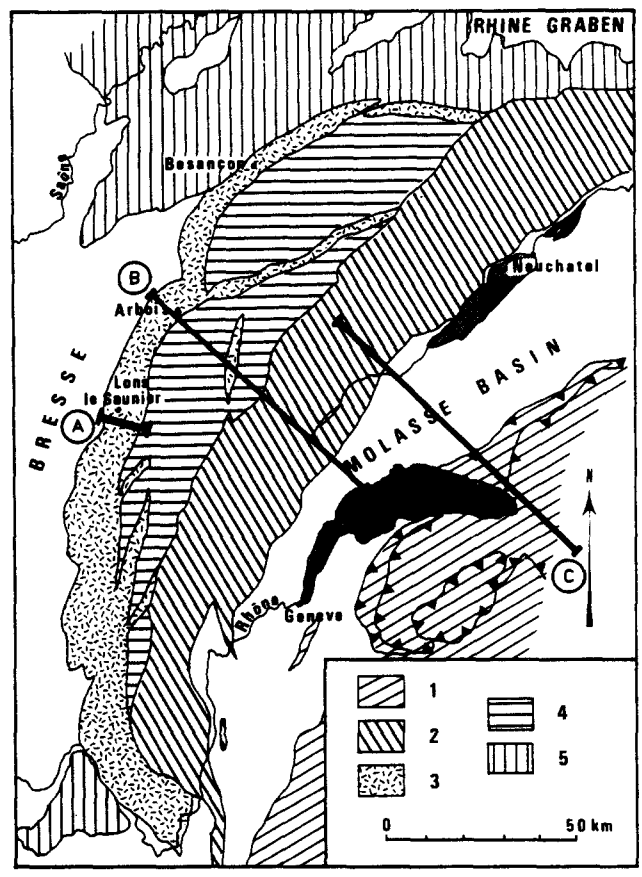

Fig. 1. Geological sketch of the Jura with the position of the cross-sections. Legend: 1, Subalpine and Préalpes domains; 2, Internal Jura, 3, 'Faisceaux' of the External Jura; 4, Weakly deformed plateau; 5, Mesozoic formations of the surrounding region; White, Tertiary basins.

Cremieu), or undisturbed gradual transitions into the outer sedimentary basins (Schwabisch Jura, Franconie).

(3) The Jura is in the Alpine foreland and its formation is linked to that of the Alps.

(4) The Alpine intracrustal thrusts and associated crustal thickening (Ménard 1979, Hsu 1979) have affected the sedimentation and the subsequent deformation of the Molasse Basin and Internal Jura.

(5) The undeformed molasse, between the Alpine front proper and the more distant deformed foreland (Jura), is a special problem to be kept in mind (Laubscher 1972).

(6) The structural patterns of the Jura in plan are more or less concentrically arranged in an arcuate pattern, with several contrasted zones of deformation; for example, the Internal Jura, the plateaux and the 'faisceaux' of the External Jura.

(7) The sedimentary cover was initially wedge shaped and heterogeneous. The composition and thickness of the sediments are determined by their position relative to the Alpine front. Near the front, the molassic sediments are very thick and massive, resting on a well-stratified Mesozoic sequence. Further to the northwest, the molasse thins and then disappears, while the Mesozoic sediments also decrease in thickness towards the northwest.

(8) This wedge-shaped composite cover rests on the eroded Hercynian basement, and begins with the evaporitic Triassic facies on which a subsequent easy décollement could have occurred.

(9) Shortening of the basement under its cover by wrench faulting or thrusting is possible but difficult to prove, since the superficial structures of the displaced sedimentary cover cannot be linked directly to deep hidden structures in the basement. Indeed, available geophysical data indicate no overthickening of the crust (Michel 1978) and a regular pre-Triassic surface dipping gently SE (Rigassi 1977b).

In order to obtain a coherent geodynamical explanation of the origin of the Jura, data on the geometry of the structures (see Appendix 1) have been analysed using the following methods. (1) Structural analyses determine the main directions of the finite deformation. (2) Construction of balanced cross-sections provides a quantitative value of the bulk shortening in the cover. (3) Vertical displacements under the Jura and the Molasse Basin have been calculated for an elastic model of the Earth's crust subjected to loading by Alpine thrust sheets. (4) The conditions inducing décollement and deformation in the heterogeneous sedimentary cover have been appraised by combining several realistic mechanical parameters.

The result of each method influences the application of the others. Thus the different methods are used iteratively, so as to control, complement, and occasionally modify the partial results obtained from individual methods (Elliott 1983). The application of all these methods has been simplified by a computerized approach, systematically used to combine the methods and to test the numerous data and possible parameters.

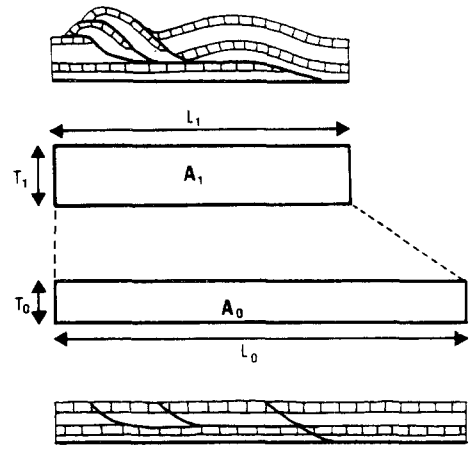

Fig. 2. Balanced cross-section techniques using the total area of the section. A section of crust of initial length L_0 and average thickness T_0 is contracted into L_1 with an average structural thickness T_1. During plane strain A_0, the initial area, is equal to A_1, the final area. Therefore, $L_1 \times T_1 = L_0 \times T_0$ and $L_0 = A_1/T_0$. A_1 is calculated by surface integration between two reference levels.

Thus several intermediate or partial solutions have been tried. When necessary, or in the case of misunderstanding previous observations, controls have been carried out in the field in several key zones.

Some of the partial solutions have already been published (Vialon *et al.* 1984, Mugnier & Vialon 1984a, 1984b) as preliminary results. Other numerous possibilities have been left out. We think the single model discussed here is the simplest one to integrate the data that we know.

BULK DEFORMATION AND DISPLACEMENT OF THE JURA COVER

We use the total area of the section to construct the balanced cross-sections (Hossack 1979) (see Fig. 2). This method has been previously proposed by Goguel (1965, fig. 101).

To calculate the bulk deformation, we use the difference between the average stratigraphic thickness (T_0) (known from drill holes and/or regional stratigraphy) and the average structural thickness (T_1) (known from the present geometry of the deformed cover above its basement). This difference is assumed to be the result of a plane strain without volume change. The initial length (L_0) of the beds is calculated from the final length (L_1) occupied by the same deformed strata

$$L_0 = L_1 T_1 / T_0. \quad (1)$$

The uncertainty in L_0 derives essentially from the geometry of the structure studied. The main causes of error (Fig. 3) are (i) unrepresentative fault attitudes seen at the surface, (ii) uncertain position of the décollement level, (iii) offset of this level by faults, (iv) uncertain initial value of the thickness T_0 and (v) bulk shear strain.

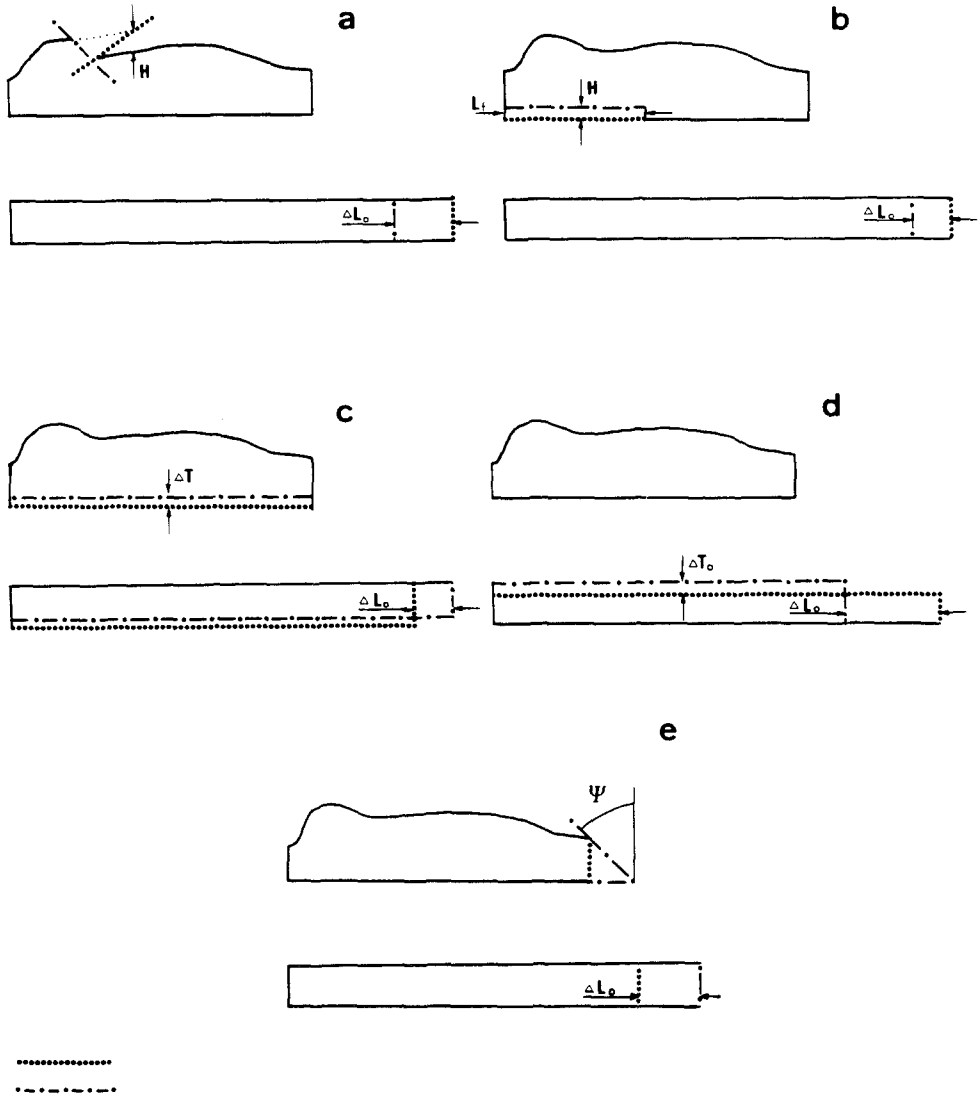

Fig. 3. Sources of error in the calculated initial length L_0 of a bed using an area-balance construction. Dotted line, assumed geometry; pecked line, true geometry. (a) Fault known only through surface outcrops. If normal fault of throw H is misinterpreted as a reverse fault, the resulting error is $\Delta L_0/L_0 = 0.7H^2/L_1T_1$. For n faults, with H_i their respective vertical throw, $\Delta L_0/L_0 = (0.7\ \Sigma_n^1 H_i^2)/L_1T_1$. (b) Fault displacing the décollement level. The induced error due to the ignorance of this displacement is $\Delta L_0/L_0 = -L_f/L_1 \times (T_1 - T_0)/T_1 \times H/T_0$. (c) Décollement level ill-defined. If it is located too deep, the induced error is $\Delta L_0/L_0 = -(T_1 - T_0)/T_1 \times \Delta T/T_0$. (d) If the stratigraphic thickness T_0 is underestimated, the induced error is $\Delta L_0/L_0 = -\Delta T_0/T_0$. (e) If a bulk shear strain is neglected, the resulting error is $\Delta L_0/L_0 = T_1/L_1 \tan \Psi$.

If there is an area change in the cross-section during the deformation, another error is added (Hossack 1979). The causes of area change are volume change (ΔV) and deformation perpendicular to the plane of the cross-section (ε_y).

The final total error is

$$\frac{\Delta L_0}{L_0} = \frac{0.7\ \Sigma_n^1 H_i^2}{L_1 T_1} + \frac{L_f}{L_1}\frac{|T_1 - T_0|}{T_1}\frac{H}{T_0} + \frac{|T_1 - T_0|}{T_1} \times \frac{\Delta T_0}{T_0} + \frac{\Delta T_0}{T_0} + \frac{T_1}{L_1}\tan \Psi + \frac{|\Delta V - \varepsilon_y|}{1 + \Delta V}, \quad (2)$$

where n is the number of faults with throws H_1 to H_n and L_f is the horizontal distance over which the décollement has been offset by a vertical distance H (Fig. 3).

The example of the Jura shows that the main error is essentially due to the estimate of the stratigraphic thickness T_0 (about 10%). The error induced by the area change is less than 5% since $\varepsilon_y = 1\%$ in the Internal Jura (Vialon *et al.* 1984). The error due to the geometry of the faults is small, about 2–5% for the faults in the displaced sheet, and 3–6% for the sole fault. The error due to the bulk shear strain is small if we study a large cross-sectional distance.

The bulk deformation of the Jura cover

The cross-section has been constructed parallel to the direction of inferred displacement, in a location which minimizes the distance between the drill holes and the

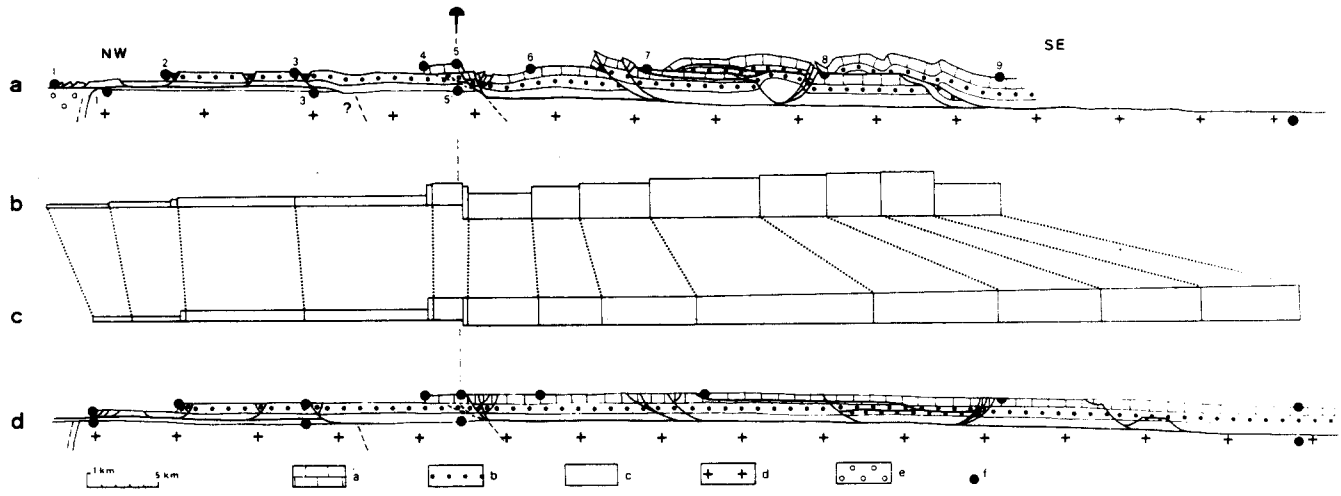

Fig. 4. Balanced and restored sections across the Jura. (a) Present geological cross-section (cross-section B on Fig. 1). Topography omitted for clarity. Positions of the reference dots: 1 to 2, 'faisceau lédonien'; 3, 'chaine de l'Heute'; 4, Mont Rivel; 5 to 6, 'faisceau de Syam'; 6 to 9, Helvetic 'faisceau'. Legend: a, Bathonian to Portlandian; b, Carixian to Bajocian; c, Muschelkalk to Sinemurian; d, Basement and its adhering Triassic. (b) and (c) Balanced cross-section constructions. The balance in the plane of the section is represented by diagrams which represent the surfaces of the layers between an upper and lower level of reference. The upper reference level is, between points 1–2, the top of the Rhetian, between points 2–4, the base of the Bathonian, and between points 4–9, the base of the Purbeckian. The lower reference level is, between points 1–5, the top of the Upper Muschelkalk, and between points 5–9, the base of the Middle Muschelkalk. (b) Shows the average structural thickness T_1. (c) Shows the reference layers restored to their initial position and thickness, keeping the area of diagrams (b) and (c) constant. In both diagrams the horizontal lengths are those of the geological cross-section cut into several segments, grouped by zones of similar geologic structure. Oblique dotted lines between diagrams (b) and (c) show the displacements of the segment limits, according to the thinning and the extension of each zone, the points 5 (shown with a 'pin' on the figure) being supposed fixed. (d) Restored cross-section before deformation. The horizontal extensions between dots, calculated using the total area of the section, are $e_{1-2} = 30 \pm 11\%$; $e_{2-5} = 4 \pm 8\%$; $e_{5-6} = -7 \pm 10\%$; $e_{6-7} = -25 \pm 9\%$; $e_{7-8} = -40 \pm 11\%$; $e_{8-9} = -41 \pm 12\%$. The horizontal displacements between basement and cover, and the horizontal extension deduced from the present cross-section using the bed lengths, are $|d_{1-1'}| = 5 \pm 1$ km; $|d_{3-3'}| > 1.6$ km. The horizontal displacements between basement and cover deduced from the balanced section construction, the reference dot n° 5 being supposed fixed, are $d_{5-5'} = 0$ km; $|d_{9-9'}| = 21 \pm 5$ km. The shortening in the basement is $e_{1'-5'} = -5\%$.

cross-section. To estimate the direction of displacement in the Internal Jura and in the Molasse Basin we have used the results of models by Laubscher (1972) and Vialon *et al.* (1984). These models imply a displacement of the Molasse Basin towards the northwest as a means of explaining (i) the arcuate fold pattern of the Jura, (ii) the fan shape of the main shortening directions inferred from structural analysis in the Jura field (Pleissmann 1972, Bonnet 1983) and (iii) the fan shape of the main stress directions inferred from earthquakes in the same area (Pavoni 1980).

In the frontal part of the Jura, where we consider gravity sliding to be the dominant driving mechanism (Mugnier & Vialon 1984b), the direction of displacement is determined by the dip direction of the plane of décollement. Along cross-section A of Fig. 1 that direction is to the west, while along cross-section B of Fig. 1 it is towards the northwest (Mugnier 1984, fig. 60). These are the stretching directions along both cross-sections.

In the inner part of the Molasse Basin, where gravity spreading could occur (Mugnier & Vialon 1984a) due to the uplift of the thrust sheets of the 'massifs cristalins externes' (Ménard & Thouvenot 1984), the direction of displacement is the dip direction of the topographic slope and the displacement direction of the thrusts of the 'massifs cristallins externes', i.e. towards the northwest.

Thus the bulk deformation of the Jura cover is analysed along a median cross-section (B on Fig. 1) of the Jura. Because of the position of the drill holes, we have unwedged the cross-section (C on Fig. 1) in the inner part of the Molasse Basin.

The bulk deformation and its relationship to structure can be described as follows.

(1) In the Internal Jura (Helvetic faisceau), the amount of shortening is about 21 ± 5 km. This implies thrusting of the cover, with an overlapping value of about 17.5 km. These values agree with the results of Laubscher (1965). The deep geometry is constrained by the drill-holes of Risoux and Chatelblanc. We have considered that the Argovian marly level and the Aalenian marly level are flats and we have balanced the line length by using the branching features, proposed by Dahlstrom (1970), Ramsay (1980) and Boyer & Elliott (1980) in another but similar context, for drawing the faults.

(2) In the 'faisceau de Syam' region (points 5–6 Fig. 4a) the assumption of a continuous and regular surface of décollement is incorrect. The Callovian/Bathonian boundary is at least 200 m higher in the plateaux than in the Toilon borehole, drilled at the top of the first anticline to the east of the 'faisceau de Syam'. Thus, if the hypothesis of a regular plane of décollement were true, there would be horizontal elongation at the east of the 'faisceau de Syam'. This is not actually observed.

Thus, it requires the introduction of irregularities in the décollement surface. Sedimentary data may be useful to determine the geometry of these irregularities. A group of Oligocene conglomerates is present in the eastern area of the faisceau. The conglomerates have a local source, contain a Jurassic component (Weber 1960, Duplaix & Guillaume 1963, Aubert 1975), and are interpreted by these authors as associated with normal fault scarps. These faults would be the main faults of the 'faisceau de Syam' as described by Guillaume (1961a). Their vertical throw is more than 800 m. To accommodate the throw of the normal faults, Mussillon (1962) and Guillaume & Guillaume (1965) have proposed that they could affect the basement. Thus we have introduced an offset in the basement, the southern part of which has been down thrown 600 ± 300 m (Mugnier 1984). During the Mio-Pliocene event, the 'faisceau de Syam' was a zone of sinistral transpression (Laubscher 1965). Guillaume (1961b) observed local thrusts with displacements towards the southeast, which uplift the plateau near the 'faisceau'. Thus we have introduced a back-thrust with a tip-line below the plateau. But other solutions are still possible: Laubscher (1965) has drawn a complex thrust system dipping NW.

(3) In the plateaux of the External Jura, drill-hole data (Valempouliere 1, 3, 101, Thesy) suggest probable shortening by reverse faults in the Muschelkalk series and extension by normal faults in the higher part of the sedimentary pile. Under these conditions, the use of total area to balance the cross-section is only possible for the beds postdating the Muschelkalk formation. For these beds there is a very little extension, observed in the 'pincées' structures (Glangeaud 1949) like the 'Heute Chain'. For the level of the Muschelkalk the shortening can be obtained by using the lengths of the beds:

$$L_0M = L_0K, \tag{3}$$

$$L_1M = L_1K - F, \tag{4}$$

where L_0M and L_0K are the initial lengths of the Muschelkalk and Keuper beds, respectively; F is the distance of overlap onto the Bresse graben, and L_1M and L_1K are final lengths of the Muschelkalk and Keuper beds, respectively. Then

$$L_0M - L_1M = L_0K - L_1K + F. \tag{5}$$

We obtain by this method a shortening of about 2 km in the Muschelkalk formation. Under the 'Heute Chain', in the middle of the external plateau (point 3, fig. 4a), the shortening due to the thrusting in the Muschelkalk formation is at least 1.6 km, according to drill-hole data (Mathis 1973).

(4) In the most external part of the plateau, the use of the total area to balance the cross-section reveals an important SE–NW horizontal extension, linked to the tectonic overlap of the Tertiary sediments in the Bresse graben by the Mesozoic rocks of the Jura. This is confirmed in the two calculated cross-sections. Thus, a new geological interpretation is proposed for this external segment (Fig. 5, located on Fig. 1, cross-section A) (Mugnier & Vialon 1984b). The balance between the total area of the section and the length of the beds is satisfied by normal listric faults. These normal faults were observed by Goguel & Bonte (1951), before the discovery of the tectonic overlap of the Bresse Tertiary by the Jura Mesozoic (Michel *et al.* 1953). This discovery is the basis of the classical interpretation with thrust and reverse faults (Le Favrais-Raymond 1962, Lienhardt 1962). The SE–NW stretching is in this way clearly expressed. A part of it is later than the Oligocene and thus cannot be due to the rift extension. The bulk thinning of the displaced cover fits the geometry of the cross-section and the field observations better than the thrusting hypothesis which implies shortening and thickening. Thus, the geometry of the Bresse borders of the Jura is very similar to the geometry of landslide structures (Seed & Wilson 1967, Voight 1973).

Cover displacement over the basement

The bulk deformation of each segment of cover allows the computation of the corresponding variations of relative displacement along the décollement level. To estimate absolute displacement of the cover, relative to its basement, the procedure is to determine a pin line and to use line-length balancing (Dahlstrom 1969).

The classic choice for the pin line, in the Jura Mountains, is the Bresse graben (Laubscher 1965). But we propose in this paper another pin line, at the eastern limit of the plateaux, for reasons discussed in the section on mechanisms controlling the décollement of the External Jura.

By reference to this pin line, the comparison between the present cross-section (Fig. 4a) and the restored undeformed pile (Fig. 4d), shows the absolute displacement of the cover. The displacement is important in the most internal part of the Jura massif (21 ± 5 km) and weakens progressively northwestward as far as Syam where we assume that it vanishes. Further northward of this fixed point, the balanced section construction requires the deep structures and the superficial structures to behave differently. The 6 km overlap onto the Bresse graben is due to a small shortening of the basement and of the deep cover, and to an extension of the superficial cover. The latter is an important factor in the frontal slide over the Bresse graben.

Lateral continuity of the structures

Cross-sections represent the structures in the plane of the section. Perpendicular to this plane structures evolve laterally. Thus, the bulk extension across a structure on a regional scale in a mountain belt could change gradually (Dahlstrom 1969).

In the present case, wrench faults of the cover, which correspond to anomalies (fault slopes, topography) of the basement surface, make the projection of structures out of the plane of the median Jura cross-section a questionable exercise. This is the case for the structure of the eastern border of the Bresse graben: south of the

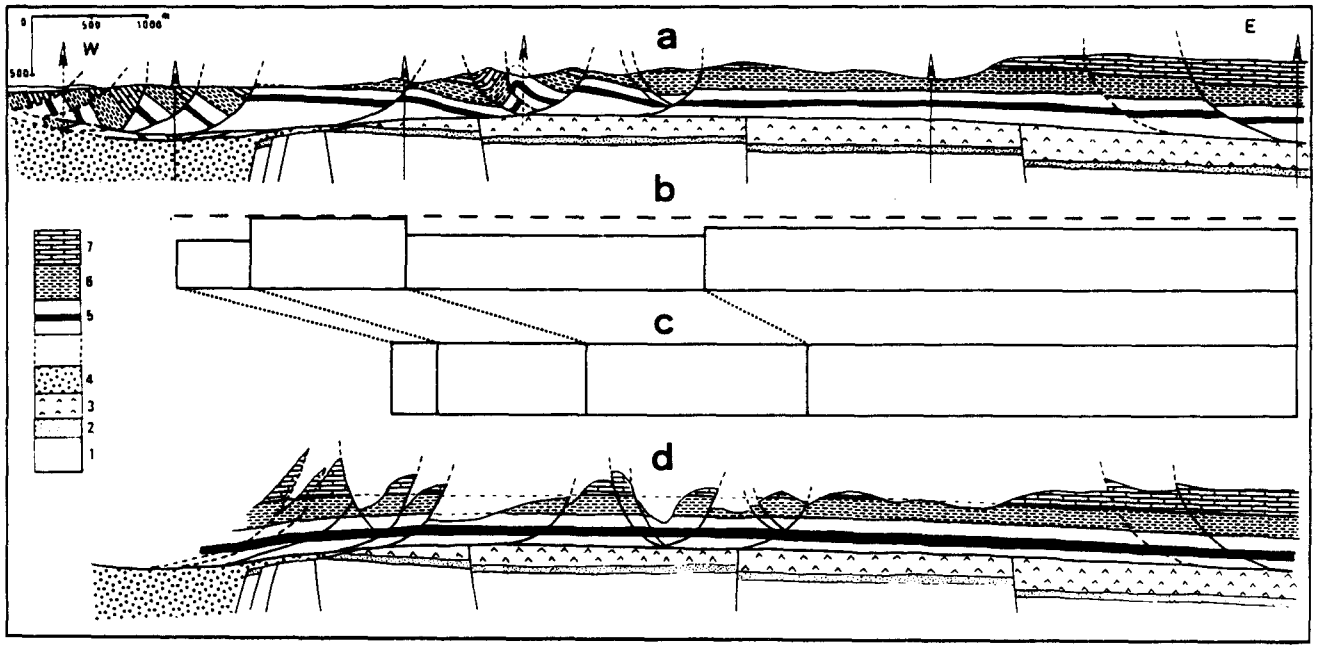

Fig. 5. Geological and balanced cross-sections of the frontal Jura in the Vignoble area ('faisceau lédonien'). (a) New interpretation where the overlap onto the Bresse graben is expressed by normal listric faults, as in a gravity landslide (Mugnier & Vialon. 1984b). Drill holes are situated either in their true positions if they are in the plane of the cross-section, or projected onto it if they are only near. The western part of the geological cross-section is in the Bresse domain where no outcrop or drill data exist. Therefore it is impossible to draw the frontal end of the overlapping structures. Overlapped formations: 1, Paleozoic which rests on a deeper crystalline basement, not shown in the drawing. Adhering Triassic with: 2, Lower Triassic; 3, Middle Triassic. Bresse Tertiary formations with steps of graben faults: 4, Mesozoic displaced cover: 5, Upper Triassic (Lettenkohle to Rhetian) with a reference layer in black; 6, Lias; 7, Dogger. (b) and (c) Balanced section constructions. The balance in the plane of the section is given by diagrams which represent the areas occupied in the plane of the section by the Triassic (5) with its reference layer (black). Diagram (b) shows the average structural thickness while a broken line represents the average stratigraphic thickness (340 m). Diagram (c) shows the reference level restored to its initial place and thickness (340 m) keeping the area of diagrams (b) and (c) constant. Other elements as in Fig. 4. (d) Restored cross-section before deformation.

median cross-section the boundary seems to be a shift of the basement surface; whereas the transform wrench fault between the Rhine graben and the Bresse graben (Laubscher 1970) forms the boundary to the north. The thrust structures of the internal Jura seem to stop against the Vuache fault in the southwest, and against the Pontarlier fault in the northeast (Aubert 1971).

VERTICAL DISPLACEMENT OF THE BASEMENT UNDER THE JURA AND THE SWISS MOLASSE BASIN

The gradual and asymmetric subsidence of the basement is unquestionably shown by the evolution of the sedimentation of the Molasse Basin ahead of the Alpine thrust front. This situation supports the interpretation of a bending of the European lithospheric plate as a result of loading on its southern border due to a pile up of Alpine thrust sheets. Generalized interpretative cross-sections of the Alps, recently proposed by Ménard (1979), Perrier & Vialon (1980) and Ménard & Thouvenot (1984) (Fig. 6), show how the subsidence of the foreland is related to the Alpine intracrustal thrusting.

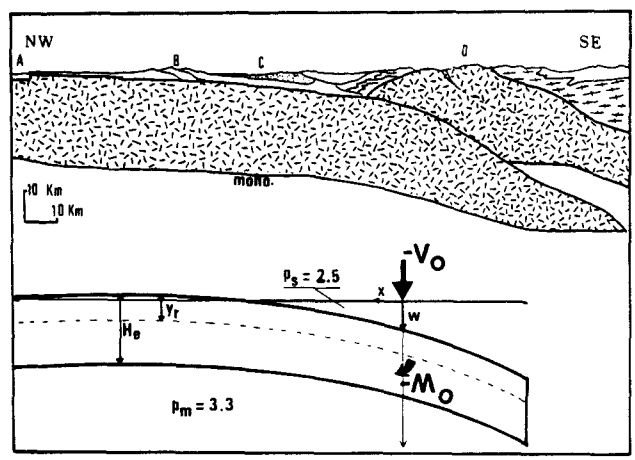

Fig. 6. Interpretative deep structural cross-section of the Alps and foreland according to Ménard & Thouvenot (1984, fig. 4). Bending model of the European plate in the foreland of the Alps deduced from the cross-section. Points on the profile: A, Bresse Graben; B, Internal Jura; C, Molasse Swiss plateau and D, Crustal thrusting thickening the crystalline basement in the Mont-Blanc region. Overloading due to Alpine intracrustal thrusts produces stresses in the section of the European plate with $x = 0$, equivalent to the action of a vertical shear force V_0 and a bending moment M_0. The part of the European plate with a positive abscissa, behaves elastically with an effective elastic thickness H_e and the vertical displacement due to bending is w. The deformation can be seen in the shape of the basement/cover interface which reacts like a passive marker, situated at a depth y_r below the topographical reference level of the plate.

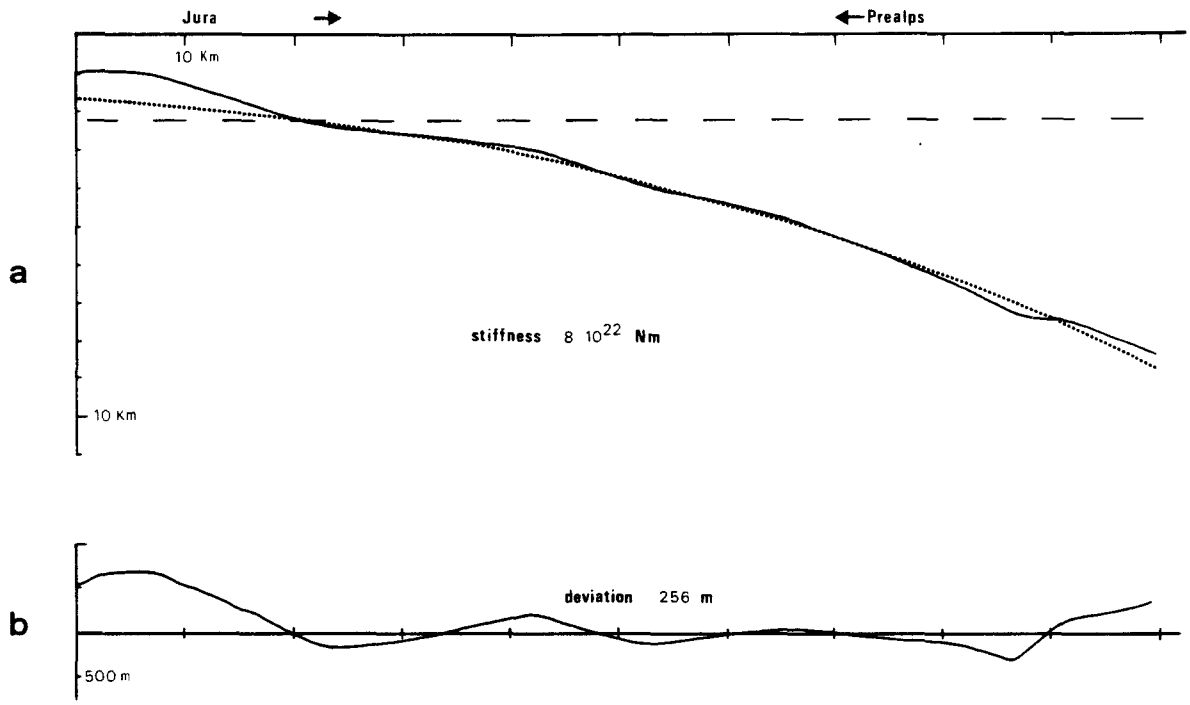

Fig. 7. (a) Flexure of the European plate in the foreland of the Alps. The continuous line represents the real profile of the basement/cover interface while the dotted line is the calculated profile with $D = 8 \times 10^{22}$ Nm. The broken line shows the position of the basement/cover interface before bending. (b) Difference between calculated and true profiles of the basement/cover interface (standard deviation = 256 m).

The bending of a lithospheric plate in subduction zones is a well-known concept. Goguel (1958) already used this concept to study regional vertical displacement patterns due to crustal faults. Price (1973) and Coward (1983) proposed a similar idea for the frontal part of mountain ranges where the forward movement of nappes produces overloading and sinking of the overlapped foreland. Likewise, Elliott (1976a) emphasized the importance of geometric analysis of foreland basins in studying the energy balance and deformation mechanisms of thrust sheets. Identically, Beaumont (1978), Karner & Watts (1983), Lyon-Caen & Molnar (1983), Royden & Karner (1984) used models of bending of an elastic plate to study the formation of foreland basins.

This hypothesis seems to be particularly suitable for the analysis of the vertical displacements shown in the Swiss molassic sediments. The mathematical solution is now a classic one (Turcotte & Schubert 1982, p. 125) and provides the basis for our calculation.

Plate stiffness

We have used the cover-basement interface derived from drill hole data (see Appendix 1) and geophysical explorations under the Jura and Swiss molassic basin as a marker for the shape of the bent plate. This interface is rather simple and not disturbed by the more superficial deformations of the cover (Baud *et al.* 1977, Rigassi 1977b, Trumpy 1980). Nevertheless the Oligocene tectonics have locally induced steps in this interface.

The stiffness of the plate is calculated from the equations quoted in Turcotte & Schubert (1982), assuming the density of the rocks of the cover below the Molasse Basin area to be $\rho_w = 2.5$, and of the mantle to be $\rho_m = 3.3$.

In order to choose the zero deflection level, taken as a reference in the subsequent bending, the variable y_r is introduced into the calculation, where y_r is the initial depth of a datum line under the initial topographic surface. In this way equation 3–151 of Turcotte & Schubert (1982) becomes

$$w(x) = \frac{\lambda^2 e^{-x/\lambda}}{2D} \times \left\{-M_0 \sin\frac{x}{\lambda} + (V_0\lambda + M_0)\cos\frac{x}{\lambda}\right\} - y_r, \quad (6)$$

where w = amplitude of vertical bending in metres (m)
x = horizontal coordinate (m)
λ = bending parameter (m)
D = stiffness of bending (Nm)
M_0 = bending moment (N)
V_0 = vertical shear (N/m)

and

$$\lambda = \left[\frac{4D}{(\rho_m - \rho_w)g}\right]^{1/4}. \quad (7)$$

The value of y_r corresponds to the thickness of the Mesozoic sedimentary pile, the top of which can be considered to be near sea level before bending. The values of (D, M_0, V_0) are not available separately. Thus the calculation consists of searching for the best combination of parameters to fit the calculated profile to the observed profile (Fig. 7, cross-section in Fig. 1). The

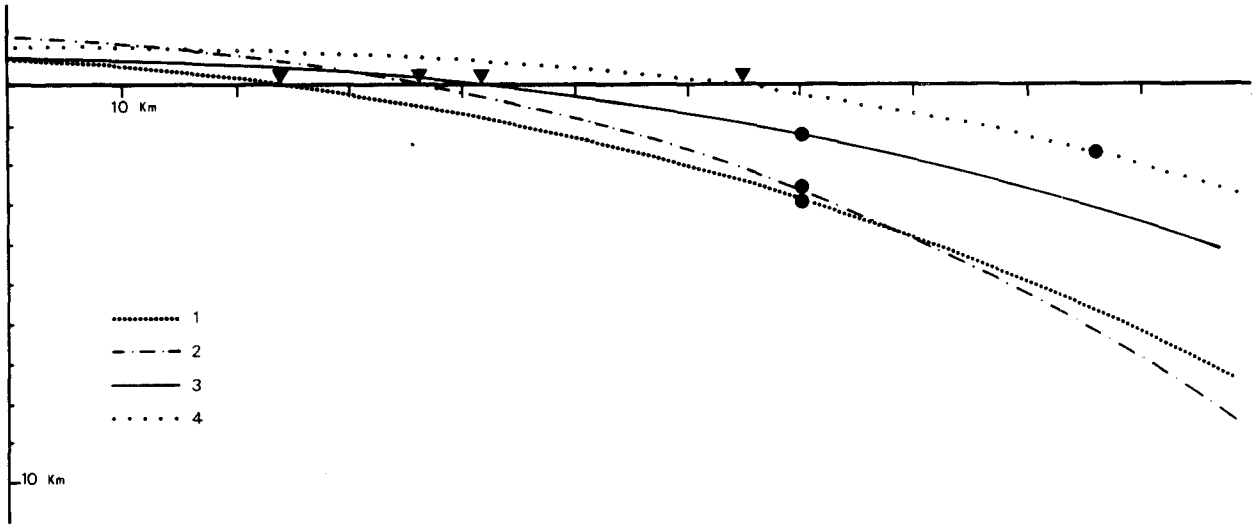

Fig. 8. Evolution of the top of the secondary formations below the Molasse Basin during the bending of the European plate. Legend: 1, Burdigalian profile; 2, Aquitanian profile; 3, Chattian profile; 4, Rupelian profile. The black triangles are the successive position with time of the shore lines. The black circles are points where the initial thickness of the successive molassic beds can be restored. Profiles calculated for a bending model of the elastic European plate with a stiffness $D = 8 \times 10^{22}$ Nm.

best fit is given by a plate stiffness of $(8 \pm 6) \times 10^{22}$ Nm. Thus the elastic thickness is about 20 km. Karner & Watts (1983), in their study of gravity anomalies, have found a stiffness of 10^{23} Nm in sections across the Western Alps. The deviation between the calculated and observed profiles (Fig. 8b) is more important below the Jura than below the Molasse Basin. Indeed, the observed profile is higher than the calculated one under the plateau. This could be due to heterogeneities inherited from Upper Paleozoic graben structures (Finck *et al.* 1984) or the Oligocene Rhine–Bresse rift system, and it shows the limitations of the homogeneous plate model.

Nevertheless we will show in the next section some geological implications of the bending model for the Alpine foreland. However the calculated values of the bending moment and the vertical shear force at the internal margin of the basin could help to constrain the deep crustal structures of the Alps.

Bulging of the crust under the Jura

The inferred uplift of the External Jura area is confirmed by sedimentary evidence; for example the presence of continental or fluviatile deposits, and of constant erosion throughout the Tertiary (Aubert 1975, Chauve *et al.* 1980). The bending of an elastic plate model may be a means of explaining part of the uplift, and another part of the uplift should be associated with the Oligocene graben formation. The model of bending produces a basin subsidence near the loading of the linear mountain front and a corresponding forebulge (Walcott 1970, Parsons & Molnar 1976, Lliboutry 1982). Thus the amplitude and position of the forebulge under the Jura may be specified under the hypothesis that the European plate is loaded at its southeastern end by Alpine thrust sheets. The sedimentation of the Molasse Basins onlaps on the forebulge (Fig. 8) and the area ahead of this line is eroded.

It is important to take the loading involved in formation of the Jura near the forebulge position into account in the calculation. This study was carried out with the computer programme of Lyon-Caen & Molnar (1983). We have determined, for different values of plate stiffness, the bending moment and the vertical shear force at the internal margin of the basin necessary to fit the calculated profile with the observed profile of subsidence in the Molasse Basin (see Table 1). According to the

Table 1. Values used in the calculation of the northwest forebulge in the European plate, flexed at its SE end by the load of the Alpine thrust sheets

	On the SE border of the Molasse Basin		Northwestward distance of the maximum height of the forebulge from the point 1′ (Fig. 4, cross-section A) (km)	Amplitude of the forebulge (m)
Plate stiffness D (Nm)	Bending moment M_0(N)	Vertical shear force V_0(Nm^{-1})		
3×10^{22}	-4.93×10^{16}	-2.2×10^{10}	+70	125
8×10^{22}	-1.14×10^{17}	-4.4×10^{11}	+55	200
13×10^{22}	-1.68×10^{17}	-7.67×10^{11}	+50	250

Rock densities used respectively for crust = ρ_w, and for mantle = ρ_m.
ρ_w: for the Jura = 2.5; for the Molasse Basin (positive altitudes only) = 2.3; (negative altitudes only) = 2.4.
ρ_m = 3.3.

different hypotheses, the top of the forebulge can be found at the present time below the Bresse graben.

The Jura domain is therefore uplifted by this bulging of the European plate associated with the down-bending of the plate due to the Alpine load, and the bulge has migrated through time towards the northeast.

Evolution of the Molasse Basin subsidence

The subsidence of the Molasse Basin is registered in the thickening and the northwest shifting of the successive deposits (Rigassi 1977a, Monnier 1979, Matter & Homewood. 1980). But erosion, deformation and scarcity of outcrops do not allow one to follow all the stages of this sedimentation. Since the model of an elastic plate seems to be a good approximation for the behaviour of the European lithosphere at the present time, we can assume it behaved similarly in the past and we can therefore try to restore the different stages of sedimentation.

We can calculate the whole of the basin profiles at different times, by taking for each stage: a NW shore line at x_0, and a deposition thickness (w_i) at another point x_i. According to equation (6) for these two points, the solution is

$$M_0 = kV_0 \tag{8}$$

$$V_0 = \frac{\dfrac{2Dw_i}{\lambda^2 e^{-x_i/\lambda}}}{-k \sin\left(\dfrac{x_i}{\lambda}\right) + (\lambda + k) \cos\left(\dfrac{x_i}{\lambda}\right)} \tag{9}$$

with

$$k = \frac{\lambda}{\tan\left(\dfrac{x_0}{\lambda}\right) - 1}. \tag{10}$$

A bending profile is therefore given by equation (6) where each parameter is determined assuming that the stiffness of the plate did not change during time.

Using the previous results concerning the bulk deformations and horizontal displacement of the Jura cover, points x_0 and x_i are chosen for different successive levels of molassic sedimentation. In each case w_i is given by drill hole data (see Appendix 1). The results of the calculation are shown in Fig. 8, and used for the balanced cross-section construction (Fig. 10).

This way of restoring the geometry of the Molasse Basin and the evolution of its filling is probably not very accurate. Nevertheless the method does take into account time variation, and presents an alternative to the classic methods of restoration. These methods are based either on the choice of a fixed and constant slope for the bottom of the sedimentary wedge or the determination of the limits of the basin by replacing the eroded material by an arbitrary thickness above the present topography.

MECHANISM CONTROLLING THE DECOLLEMENT AND THE DEFORMATION OF THE JURA COVER

As seen above, the sedimentary cover of the Jura, in front of the Alpine thrust sheets, is deformed during sliding as a thin-skinned thrust system. The cover is displaced towards the NW over a basement which is bent towards the origin of the displacement. This interpretation must now be checked against realistic mechanical models which could explain the mechanism controlling the thrust tectonics (Siddans 1984).

Three types of mechanism could reasonably describe the displacement of the Jura cover (Merle 1984). Mathematical models based on simplified mechanical hypotheses will be used for this. Despite the simplification, the use of analytical models is justified in the study of the motion of thrust sheets, because "they allow one to separate conclusions based largely upon the statics of thrust sheets from results which depend upon assumption about special laws of sliding along the base of thrust sheets" (Elliott 1976b).

According to the different geometries of the displaced sheet and the values of the assumed mechanical parameters (Mugnier & Vialon 1984a) (Fig. 10), restrictions on the applicability are imposed eventually leading to the employment of one model or another. Thus, the geometrical and mechanical constraints obtained here can be used to discriminate between different mechanisms proposed to explain the displacement and the deformation.

Mathematical description of the models

The deformation and movement of the cover of the Jura over a passive basement can be assumed to be similar to that of a superficial thrust sheet. The shear stress induced at the décollement level of such a sheet must be equal to or greater than "the shear strength under natural conditions of the rocks" (Elliott 1976b, p. 950). In the different possible models this condition is written as follows (see Fig. 9 for the definition of the parameters).

Model (a), gravity sliding (Hubbert & Rubey 1959):

$$\rho g H \sin \beta > K_b. \tag{11}$$

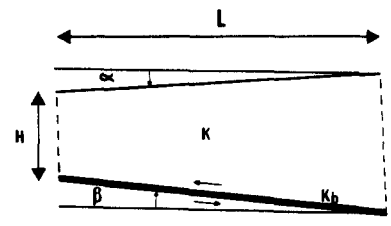

Fig. 9. Simplified geometric shape of a thrust sheet in cross-section. H, thickness; β, basal slope; α, topographical slope; K, yield strength of the wedge; K_b, yield strength of the base of the sheet.

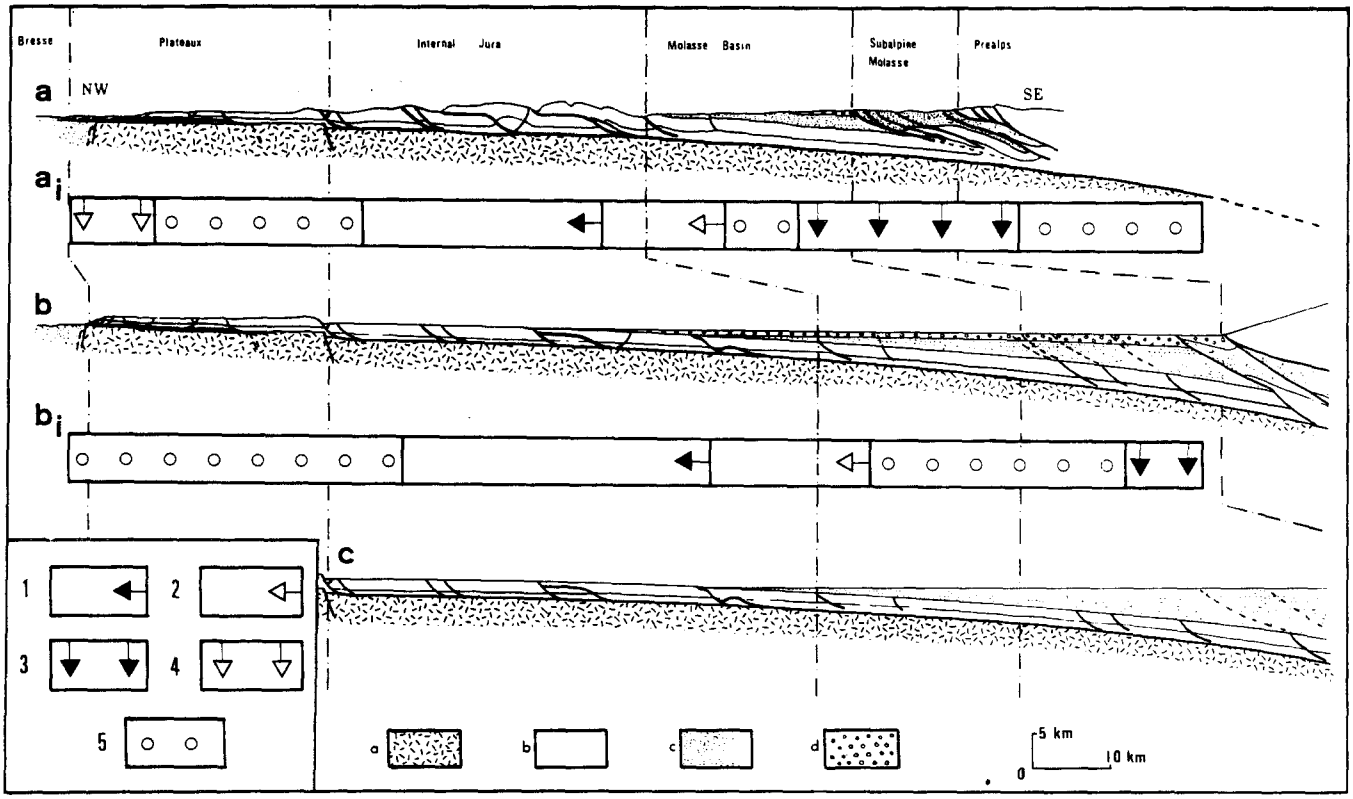

Fig. 10. Restored evolution of the Molasse Basin wedge and mechanisms of deformation and décollement of the cover relative to its basement. (a) Present geometry of the geological cross-section. The structures are those shown in Fig. 4 for the Jura and from Baud *et al.* (1977) for the Molasse Basin. (b) and (c) Restored cross-sections for Burdigalian (b) and for Chattian (c). The vertical displacements are deduced from Fig. 8 and the horizontal displacements from Fig. 4. Legend: a, pre-Triassic basement; b, Mesozoic formations; c, old molassic formations up to Chattian included; d, molassic formation between Chattian and Helvetian. a_i and b_i: mechanisms of décollement; a_i, at the end of deformation; b_i, when the deformation began. The different possible mechanisms (see text), are: 1, horizontal push with superficial deformation; 2, horizontal push without superficial deformation (rigid slipping); 3, gravity spreading; 4, gravity sliding; 5, domains where no tested model is applicable. The values of the mechanical parameters used are: K, yield strength of the entire sedimentary wedge = 35 MPa. K_b, yield strength of the basal part of the displaced sheet = 3 MPa (tan 10° σ_N for the border of the Bresse graben). D, stiffness of the bent plate: 8×10^{22} Nm.

Model (b), gravity spreading (Elliott 1976b):

$$\rho g H \alpha > K_b \tag{12}$$

with

$$\rho g H \gg K_b \tag{13}$$

$$L > 5H \tag{14}$$

$$\alpha + \beta < 5^0. \tag{15}$$

Model (c), horizontal pushing (Chapple 1978):

$$2\beta K + \rho g H \alpha > K_b \tag{16}$$

with

$$\frac{H}{L} \gg \beta \tag{17}$$

$$\alpha < 5^0 \tag{18}$$

$$\beta < 5^0. \tag{19}$$

The thrust sheet is superficially deformed in this case only if equation (15) is strictly satisfied. Otherwise there is no deformation on the topographic surface.

Value of the parameters in the Alpine foreland

The cross-section is divided into several segments and in each the deformation of the sheet is compared with the result of the calculation. For each case the parameters are combined in order to fit the mechanical models with the observations in the closest possible manner. The geometrical parameters are determined from the geometry of the previously constructed balanced cross-sections. The undeformed state of the region is given by a restored cross-section for the Middle Miocene (see above and Fig. 10), because this period preceded the Jura formation, which may have taken place between the late Middle Miocene and Pliocene (Burgisser 1979). Table 2 gives values of the geometrical parameters for segments characteristic of the different contrasting deformation zones of the thrust sheet.

The mechanical parameters K and K_b are respectively the shear strength of the entire sheet and the shear strength of the basal décollement level. They are averages in space and time of the natural deformational properties of the rocks of the displaced sheet and of the décollement level, respectively. The natural deformation of these rocks is impossible to reproduce completely under laboratory conditions because of differences of scale. Furthermore, the theory of the natural deformation has not been completely studied. The choice of the values of K and K_b is thus empirical but should be

Table 2. Values of the parameters controlling the décollement

	Final state					Initial state				
				with K = 35 MPa					with K = 35 MPa	
	$\sin\alpha$ (%)	$\sin\beta$ (%)	H (m)	$-\rho g H \sin\beta$ (MPa)	$2\beta K + \rho g H\alpha$ (MPa)	$\sin\alpha$ (%)	$\sin\beta$ (%)	H (m)	$-\rho g H \sin\beta$ (MPa)	$2\beta K + \rho g H\alpha$ (MPa)
Bresse border (dot 2, fig. 4)	3	−2	600	0.3	—	1	−2	1200	0.6	—
Plateaux (dot 3, fig. 4)	1	1	1000	—	0.9	0.5	1	1300	—	0.8
Internal Jura (dot 7, fig. 4)	2.5	2	2500	—	3	0	3	2500	—	1.4
Molasse Basin (dot 9, fig. 4)	1	3	3000	—	3	0	5	3800	—	3.5

restricted to the following values according to different studies on thrust mechanisms (Goguel 1945, Hubbert & Rubey 1959, Elliott 1976b, Chapple 1978, Laubscher 1979, Muller & Briegel 1980, Siddans 1984).

$$20 \text{ MPa} < K < 150 \text{ MPa}$$
$$0.5 \text{ MPa} < K_b < 5 \text{ MPa}.$$

We have tested different values of K and K_b (Mugnier & Vialon 1984a). For the full range of values specified above the emplacement of the structures of the Internal Jura and its nearby mollassic border requires a horizontal push (model c), since the centre of gravity of the cover sheet of the Internal Jura has been uplifted during the deformation. Thus, K and K_b can be obtained directly by analysis of the natural deformation of the Internal Jura. Indeed the present geometry of the surface of the Jura is probably like an equilibrium profile of plastic deformation (Chapple 1978). Thus, K_b is for the Internal Jura

$$K_b = 2\beta_j K + \rho g H_j \alpha_j \quad (20)$$

and for the NW border of the molassic basin

$$K_b = 2\beta_p K + \rho g H_p \alpha_p. \quad (21)$$

The solution of these equations gives K_b = 3 MPa and K = 35 MPa.

Goguel (1945) found a similar value for K_b. We may consider the value for K (35 MPa) as the highest value of the deviatoric stress in the Alpine frontal sedimentary wedge, since the Internal Jura is the most deformed part of this wedge. We use these values as the basis for a discussion, in the next section, of the mechanisms controlling the décollement.

Evolution of the mechanisms controlling the décollement and the displacement of the thin-skinned thrust sheet of the Jura

The purpose of this section is to find which mechanical models allow shear along the footwall of the sedimentary wedge. We have calculated the value of the shear stress on the thrust plane in the different models with the values of the parameters determined above (see Table 2). With K_b = 3 MPa this calculation shows the following (see Fig. 10).

(1) Gravity spreading is only possible, i.e. equation (12) is satisfied, in the internal domain of the so-called thrusted molasse. The triggering effect is the loading due to Alpine thrust sheets.

(2) A horizontal push can explain the décollement, i.e. equation (16) is satisfied, in the northwestern part of the Swiss molasse and the nearby Internal Jura.

(3) The initial wedge shape of the Internal Jura is insufficient to cause forward propagation of the décollement. The horizontal shortening of the cover sheet increases the wedge shape and allows propagation of the décollement (at the present time, equation (16) is satisfied, even though at the initial stage it is not).

(4) Equations (11), (12) and (16) are not satisfied in the External Jura. The models, with these parameters, do not explain the décollement of this part of Jura. Thus in the next section we discuss the possibility that the External Jura cover is not a thin-skinned thrust.

A NEW INTERPRETATION OF THE MECHANISMS CONTROLLING THE DECOLLEMENT OF THE EXTERNAL JURA

Point (4) of the previous section does not agree with Laubscher's now classical interpretation (Laubscher 1965, 1980) of the whole Jura as a thin-skinned thrust and fold belt. As a result, we have analysed successively the geometry of the displaced sheet, the behavior of the décollement level and other possible mechanisms which could control the décollement of the External Jura. We propose an alternative model to the thin-skinned thrust model.

The geometry of the displaced sheet

The drill holes in the external part of the Jura show that there is a décollement in the lower Keuper level. The overlap of the Jura cover onto the Bresse graben shows a displacement of several kilometers along this décollement. But in the internal margin of the plateaux, there is no drill hole to prove the décollement. The geometries, proposed in this paper or by Laubscher (1965), below the 'faisceau' of Syam both show that the thin-skinned thrust of the Alpine foreland dies out there. Indeed, the step basement fault that we propose below the 'faisceau' cannot be a ramp for the main thrust, since

there is weak deformation where the hangingwall ramp would be. The complex structure proposed by Laubscher (1965) is rather similar to the more external structure, where the displacement vanishes of the Cordilleran foreland thrust in the Canadian Rocky Mountains (Price 1981).

We have analysed (Mugnier & Vialon 1984a) the respective influence of the geometrical parameters on the possible mechanism controlling the décollement of the sedimentary wedge. It seems that the décollement level must be seriously weaker under the External Jura than under the Internal Jura: all the geometrical parameters (H, α, β) are smaller in the External Jura than in the Internal Jura. Indeed, the Internal Jura was already wedge-shaped before the deformation, and continued deformation served to strengthen this wedge. The External Jura must have experienced very little deformation, since its units retain a uniform thickness across the zone. Moreover, the displaced cover is thinner in the External Jura than in the Internal Jura; the main décollement levels are respectively the base of lower Keuper and the base of the middle Muschelkalk.

The behaviour of rocks in the décollement level

To know if our mechanical parameters are realistic we may attempt to compare the natural deformation with experimental studies of the behaviour of rocks. At the base of the lower Keuper, the main décollement is an interstratified unit of anhydrite, dolomite and marl; and the lower Keuper itself is a thick salt horizon.

The deformation of this type of interstratified unit has been well described by Laubscher (1975), and it is clear that pressure-solution phenomena are important. But there is no published work to our knowledge about the experimental behaviour of the system anhydrite plus water at the state of pressure and temperature existing below the External Jura, i.e. 40–70°C and 15–50 MPa. Muller & Briegel (1980) have studied dry anhydrite creep under higher temperature and pressure states, close to the ones which exist below the Molasse Basin. They have proposed a flow law for the behavior of anhydrite. The deformation pattern of their finite element model fits well with the observations when they used the strength of the anhydrite calculated in the flow law with the natural estimated displacement rate (2–3 mm/year) of the Molasse Basin.

Heard & Rubey (1966) have studied the behaviour of gypsum at slightly higher temperature states than those in the External Jura. They have shown the importance of the reaction gypsum → anhydrite + water, which gives an abnormally high fluid pressure with an increase in temperature. This reaction could explain the décollement under the Molasse Basin and the Internal Jura, where the temperature increases with the overburden thickness because of the sedimentation. But in the External Jura the temperature in the décollement level has probably decreased since there was continuous erosion in this area during the Tertiary, and since we have no reason to expect an increase of the geothermal gradient in the Jura during this period.

Nevertheless, there is at present a high pressure of fluids under the external Jura, where the ratio λ_f (i.e. fluid pressure/ρgH) reaches 0.45 in the drill hole of Perrigny. This is due to gas found by drill holes in Lettenkhole level. This fluid pressure could explain the décollement of the External Jura. If the reduced shear strength of the rocks is due to failure caused by high pressure of fluid, the criterion of Terzaghi (1923) can be used (Hubbert & Rubey 1959)

$$K_b = C + \mu(1 - \lambda_f)\rho gH \qquad (22)$$

where C is the cohesive strength and μ the coefficient of internal friction.

To have values of K_b which permit displacement by push (i.e. equation 16 is satisfied), λ_f must be higher than 0.85 below the plateaux; and to permit gravity sliding near the Bresse graben λ_f has to reach 0.9 (see Table 2). The difference between the fluid pressure necessary to permit décollement and that existing now could be due to a decrease of fluid pressure during displacement, which would have stopped displacement. Such high fluid pressures are known in oil fields (Hubbert & Rubey 1959), and they may have been reached in the External Jura with the help of erosion. Indeed, erosion decreases the lithostatic pressure whereas fluid pressure remains at high values below the impervious strata. Therefore the mechanical erosion along the Bresse trough at the end of the Miocene (Chauve *et al.* 1980) could have had an important triggering effect for gravity sliding of the cover in this area.

Gravity sliding of the Jura cover over the Bresse graben and basement shortening below the plateaux

In the more external part of the plateaux, balanced cross-sections reveal an important SE–NW horizontal extension. This extension can be explained by a gravity sliding model, since the altitude of the centre of gravity has decreased during deformation and the high fluid pressures necessary for the décollement of the plateaux satisfy equation (11). Thus this 4 km of extension, the major part of the 6 km of overlap, can be attributed to the mechanism of gravity sliding (Mugnier & Vialon 1984b).

Part of the other 2 km can be due to a shortening of the basement (Winslow 1981) below the plateaux. The idea that a shortening of the basement is possible is not a new one (Pavoni 1961), and two recent focal mechanisms of earthquakes corroborate this shortening. One earthquake resulted from strike-slip movement at a depth of 15 km (Dorel *et al.* 1983), and others were associated with thrust movement at a depth of 5-6 km (Pavoni & Peterschmitt 1974). A little shortening of the basement (~5%) could induce 2 km of displacement and could explain all the décollement of the External Jura. This enables the cross-section of Fig. 4 to be balanced with the pin line in the southeast part of the plateaux, near the Internal Jura.

This small shortening of the basement, and the positioning of the pin line, may agree with the regional pattern of the External Jura. In the northern part, thrusts are observed in the 'faisceaux Salinois' and 'Bisontin'. The bulk shortening is small, not more than a few kilometers (see the cross-section in Caire 1963), and is associated with sinistral transpression in the basement, between the Bresse graben and the Rhine graben (Laubscher 1970, Bergerat 1977, Illies 1981). In the southern part of the External Jura, the overlap of the Jura cover onto the Bresse graben can also be observed in drill holes (Michel *et al.* 1951). Here the overlap is less than 2 km. Moreover, the plateaux of the External Jura no longer exist in the southern Jura, as the thrust and fold belt of the Internal Jura reaches the Bresse graben.

A COMPOSITE MODEL OF THE JURA DEFORMATION

Along a cross-section of the Jura between the Alpine front and the Bresse trough, deformation can be explained by the juxtaposition of several successive and complementary mechanisms. Their relative positions give a good idea of the gradual weakening of orogenic effects in the foreland of a collision range of mountains such as the Alps. However, the particular boundary conditions of the studied cross-section (crustal thrusting and grabens to the northwest) are on a continental scale. The local conditions determine local mechanisms which are described by different models: horizontal pushing, gravity spreading and gravity sliding.

The Alpine crustal thrusts define the initial geometry of the foreland. Significant internal relief in the southeast is due to the basement thrust sheet and consequent flexure below the Molasse Basin, which results in the formation of a sedimentary wedge thinning to the northwest and finishing with onlap on the forebulge. As this geometry is developed, deformation starts and gradually progresses northwestwards as a thin-skinned thrust belt, leading to the formation of successive contrasting structures in concentric zones.

Due to the load of the Alpine thrust sheets, gravity spreading occurs in the internal molasse. Because of the existence of a ductile Triassic level at the basement/cover interface, the forces are transmitted towards the northwest by a rigid slipping of the external molasse. This movement induces a horizontal pushing at the southeast border of the Internal Jura where the deformation occurred by horizontal indentation. However deformation and décollement do not seem to have propagated below the External Jura. Indeed, the cover is thinner, and the slopes of the topographic surface and of the basement/cover interface are smaller, in the External Jura than in the Internal Jura. These facts prevent the propagation of a thin-skinned thrust system initiated at the border of the Alps. Basement faults, probably resultant from Oligocene tectonics provide an adequate explanation to balance the area of the cross-section. Furthermore the presence of these normal faults provides another reason for stopping the thin-skinned thrust mechanism propagating in the External Jura.

Towards the external part of the Jura there is very little deformation and décollement and none at all in some parts of the plateaux area. However a small amount of shortening may exist in the basement due to deep wrench faults or reactivation of the extensional features that operated in the Oligocene. In the frontal part, gravity sliding produced overlap onto the eastern part of the Tertiary formation of the Bresse graben. The migration towards the northwest of the forebulge in the European plate, the local dip of the surface of décollement toward the northwest, the mechanical erosion at the border of the Bresse graben, and the correlated overpressure of fluids, could all have controlled this last and distant consequence of the Alpine orogenesis.

CONCLUSION

It is thus clear, that several mechanisms of deformation and displacement, successive in space, explain the diminution of deformation in the foreland of a plate-collision type orogeny such as occurred in the Alps. According to several tests, such as the focal mechanisms of earthquakes, structural analysis in the field, kinematic constructions with balance cross-section techniques, and tests with simple but realistic mechanical models, this interpretation of a median section through the Jura holds together well. This study makes it evident, however, that a unique explanation like the thin-skinned thrust model is not sufficient, even along a single cross section of a mountain chain which seems as simple as the Jura. It also means that the model that we propose cannot be extrapolated to other sections of the Jura, as there may be changes in thickness of the sediments, in rock behavior, or in the boundary conditions.

We wish to further emphasize two final points: (1) the power of the technique of balanced cross-sections in testing the consistency of an assumed geometry and a kinematic model; and (2) the importance of understanding lithospheric structures at depth if one is to explain superficial deformations.

Acknowledgements—We are deeply indebted to Professor J. P. Schaer for his interest in our work. We thank Professor H. Laubscher for his helpful criticisms of our preliminary publications. We are grateful to H. Lyon-Caen, and the two anonymous reviewers for their constructive comments on the manuscript, and to J. P. Platt, W. Shea, R. Gillchrist, N. Harwood, for their help in improving our English.

REFERENCES

Aubert, D. 1975. L'évolution du relief jurassien. *Eclog. Geol. Helv.* **68**, 1–64.

Aubert, D. 1971. Le Risoux, un charriage jurassien de grandes dimensions. *Eclog. Geol. Helv.* **64**, 151–156.

Baud, A., Burri, M., Caron, C., Dalpiaz, G. V., Escher, A., Gosso, G., Homewood, P., Masson, H., Savary, B., Schaer, J. P. & Weidmann, M. 1977. Coupe synthétique Besançon—Zone d'Ivrea au 1/200.000. Prog. 3ème Cycle Géol. Str. lect. notes. Inst. géol. Lausanne.

Beaumont. C. 1978. The evolution of sedimentary basins on a visco-elastic lithosphere. Theory and examples. *Geophys. J.R. astr. Soc.* **55**, 471–497.

Bergerat, F. 1977. Fracturation de l'avant pays jurassien. *Revue Géogr. phys. Géol. dyn.* **19**, 325–337.

Bonnet, J. L. 1983. Etude du poinçonnement d'une série stratifiée, par le déplacement d'une écaille chevauchante. Thèse 3ème Cycle. Grenoble Univ.

Boyer, S. E. & Elliott, D. 1982. The geometry of thrust systems. *Bull. Am. Ass. Petrol. Geol.* **66**, 1196–1230.

Burgisser, H. 1979. Sedimentologie der oberen Süsswasser Molasse. Ph.D. thesis, ETH Zürich.

Caire, A. 1963. Problèmes de tectonique et de morphologie jurassiennes. In: *livre mém. Prof. P. Fallot. Soc. Géol. Fr.*, 105–158.

Chapple, W. 1978. Mechanics of thin-skinned fold and thrust belts. *Bull. geol. Soc. Am.* **89**, 1189–1198.

Chauve, P., Enay, R., Fluck, P. & Sittler, C. 1980. Vosges, Fossé rhénan, Bresse, Jura. *Géologie des pays européens*, Dunod Paris, 357–431.

Coward, M. P. 1983. Thrust tectonics, thin-skinned or thick-skinned and the continuation of thrusts to deep in the crust. *J. Struct. Geol.* **5**, 113–125.

Dahlstrom, C. D. A. 1969. Balanced cross-sections. *Can. J. Earth Sci.* **6**, 743–757.

Dahlstrom, C. D. A. 1970. Structural geology in the eastern margin of Canadian Rocky Mountains. *Bull. Can. Petrol. Geol.* **18**, 332–406.

Dorel, J., Frechet, J., Gagnepain-Beynex, J., Haesslek, H., Lachaize, M., Madariaga, R., Modiano, T., Pascal, G., Philip, H., Rouland, D. & Wittlinger, G. 1983. Focal mechanism in metropolitan France and the Lesser Antilles. *Ann. Geophys.* **1**, 299–306.

Duplaix, S. & Guillaume, S. 1963. Etude stratigraphique et minéralogique de formations tertiaires du Jura. *Revue Géogr. phys. Géol. dyn.* **5**, 37–54.

Elliott, D. 1976a. The energy balance and deformation mechanism of thrust sheets. *Phil. Trans. R. Soc.* **A283**, 289–312.

Elliott, D. 1976b. The motion of thrust sheets. *J. geophys. Res.* **81**, 949–963.

Elliott, D. 1983. The construction of balanced cross-sections. *J. Struct. Geol.* **5**, 101.

Finck, H. P., Ansorge, J., Mueller, S. & Sprecher, C. 1984. Deep crustal reflection from a vibroseis survey in northern Switzerland. *Tectonophysics* **109**, 1–14.

Glangeaud, L. 1949. Les caractères structuraux du Jura. *Bull. Soc. géol. F.* **19**, 669–688.

Goguel, J. 1945. Les déformations de l'écorce terrestre. *Mém. Carte géol. France* **41**, 1–530.

Goguel, J. & Bonte, A. 1951. Une interprétation tectonique de la zone du Vignoble. *Bull. Soc. géol. Fr.* **49**, 798–802.

Goguel, J. 1958. L'influence des failles et autres irrégularités de l'écorce sur la compensation isostatique dans l'hypothèse de la régionalité. *Ann. Geophys.* **14**, 1–29.

Goguel, J. 1965. *Traité de tectonique*. Masson. Paris.

Guillaume, A. 1961a. La partie méridionale du faisceau de Syam. *Bull. Service carte géol. Fr.* **264**, 49–64.

Guillaume, A. 1961b. Relations et évolution morphotectonique des plateaux centraux et de la Haute Chaîne du Jura dans la région de Champagnole–Morez. *Revue Géogr. phys. Géol. dyn.* **4**, 103–112.

Guillaume, A. & Guillaume, S. 1965. Notice de la carte géologique Champagnole 1/50.000. *Service carte géol. Fr.*

Heard, H. C. & Rubey, W. W. 1966. Tectonic implications of gypsum dehydration. *Bull. geol. Soc. Am.* **77**, 741–760.

Hossack, J. R. 1979. The use of balanced cross-sections in the calculation of orogenic contraction: a review. *J. geol. Soc. Lond.* **136**, 705–711.

Hsu, K. J. 1979. Thin-skinned plate tectonics during neo-Alpine orogenesis. *Am. J. Sci.* **279**, 353–366.

Hubbert, M. D. & Rubey, W. W. 1959. Role of fluid pressure in mechanics of overthrust faulting. *Bull. geol. Soc. Am.* **70**, 115–166.

Illies, H. J. 1981. Mechanism of graben formation. *Tectonophysics* **73**, 249–266.

Karner, G. D. & Watts, A. B. 1983. Gravity anomalies and flexure of the lithosphere. *J. geophys. Res.* **88–B12**, 449–477.

Laubscher, H. P. 1965. Ein kinematisches Modell der Jurafaltung. *Eclog. geol. Helv.* **58**, 232–318.

Laubscher, H. P. 1970. Grundsätzliches zur Tektonik des Rheingrabens. *Int. Upper Mantle Proj. Sci. Rep.* **27**, 79–87.

Laubscher, H. P. 1972. Some overall aspects of Jura dynamics. *Am. J. Sci.* **272**, 293–301.

Laubscher, H. P. 1975. Viscous components in Jura folding. *Tectonophysics* **27**, 239–254.

Laubscher, H. P. 1979. Elements of Jura kinematics and dynamics. *Eclog. Geol. Helv.* **72**, 467–483.

Laubscher, H. P. 1980. Die Entwicklung des Faltenjuras. Daten und Vorstellungen. *N. Jb. Geol. Paläont. Abh.* **160**, 289–320.

Lefavrais-Raymond, A. 1962. Contribution à l'étude géologique de la Bresse d'après les sondages profonds. *Mem. Bur. Rech. Géol. Min. Fr.* **16.**

Lienhardt, G. 1962. Géologie du bassin houiller stéphanien du Jura et ses morts terrains. *Mém. Bur. Rech. géol. min. Fr.* **9**, 1–449.

Lliboutry, L. 1982. *Tectonophysique et géodynamique*. Masson, Paris.

Lyon-Caen, N. & Molnar, P. 1983. Constraints on the structure of the Himalaya from an analysis of gravity anomalies and a flexural model of the lithosphere. *J. geophys. Res.* **88–B10**, 8171–8191.

Mathis, M. 1973. La chaine de l'Heute (Jura). Thèse 3° *cycle*, Besançon University.

Mattauer, M. 1973. *Les déformations des matériaux de l'écorce terrestre*. Hermann, Paris.

Matter, A. & Homewood, P. 1980. Flysch and Molasse of Western and Central Switzerland. *An Outline of the Geology of Switzerland. Schweiz. Geol. Kom.* **5**, 261–293.

Ménard, G. 1979. Relations entre structures profondes et structures superficielles dans le Sud-Est de la France. Essai d'utilisation des données géophysiques. Thèse 3° Cycle, Grenoble Univ.

Ménard, G. & Thouvenot, F. 1984. Ecaillage de la lithosphère européenne sous les Alpes Occidentales: arguments gravimétriques et sismiques liés à l'anomalie d'Ivrea. *Bull. Soc. géol. Fr.* **26**, 875–884.

Merle, O. 1984. Déplacement et déformation des nappes superficielles. *Revue Géogr. phys. Géol. dyn.* **251**, 3–17.

Michel, P., Appert, G. & Lavigne, J. 1951. Sondage, R. A. P. du Mont Mezon et du Revermont. *Bull. Soc. géol. Fr.* **1**, 819–821.

Michel, P., Appert, G., Lavigne, J., Lefavrais, A., Bonte, A., Lienhardt, G. & Ricour, J. 1953. Le contact Jura-Bresse dans la région de Lons-le-Saunier. *Bull. Soc. géol. Fr.* **3**, 593–611.

Michel, B. 1978. La croûte entre la vallée du Rhin et la vallée du Rhône: interprétation de profils sismiques et résultats structuraux. Thèse 3° Cycle, Paris VII, University.

Monnier, F. 1979. Corrélations minéralogiques et diagenèse dans le bassin molassique suisse. Thèse, Neuchâtel University.

Mugnier, J. L. 1984. Déplacements et déformations dans l'avant-pays d'une chaîne de collision. Méthodes d'études et modélisation. Exemple du Jura. Thèse Dr. Ing., Grenoble University.

Mugnier, J. L. & Vialon, P. 1984a. Les mécanismes de mise en place des nappes de chevauchement superficielles. Application des modèles analytiques au jura. *Bull. Sci. géol. Strasbourg* **3**, 77–87.

Mugnier, J. L. & Vialon, P. 1984b. The mechanisms of overlapping of the Bresse graben by the Jura formations in the Vignoble area (France). *Tectonophysics* **106**, 155–163.

Muller, H. W. & Briegel, U. 1980. Mechanical aspect of the Jura overthrust. *Eclog. geol. Helv.* **73**, 239–250.

Mussillon, C. 1962. Etude géologique de la région de Syam (Jura). Thèse 3° Cycle. Besançon University.

Parsons, B. & Molnar, P. 1976. The origin of outer topographic rises associated with trenches. *Geophys. J. R. astr. Soc.* **45**, 707–712.

Pavoni, N. 1961. Faltung durch horizontal Verschiebung. *Eclog. geol. Helv.* **54**, 515–534.

Pavoni, N. & Peterschmitt, E. 1974. Das Erdleben von Jeurre vom 21 Juni 1971 und seine Beziehungen zur Tektonik des Faltenjura. In: Approaches to Taphrogenesis (edited by Illies, J. H. & Fuchs, K.), 322–329.

Pavoni, N. 1980. Stresses inferred for fault plane solutions of earthquakes. *Rock Mechanics* (Suppl.) **9**, 63–68.

Perrier, G. & Vialon, P. 1980. Les connaissances géophysiques sur le Sud-Est de la France. Implications géodynamiques. *Géol. Alpine* **56**, 13–20.

Plessmann, W. 1972. Horizontal-Stylolithen im französisch-schweizerischen Tafel und Faltenjura und ihre Einspassung in den regionalen Rahmen. *Geol. Rdsch.* **61**, 332–347.

Price, R. A. 1973. Large scale gravitational flow of supracrustal rocks, southern Canadian Rockies. In: *Gravity and Tectonics* (edited by Scholten, R. & De Jong, K.) Wiley, New York, 491–501.

Price, R. A. 1981. The Cordilleran foreland thrust and fold belt in Southern Canadian Rocky Mountains. In: *Thrust and Nappe Tectonics* (edited by McClay, K. and Price, N. J.) *Spec. Publs geol. Soc. Lond.* **9**, 427–449.

Ramsay, J. R. 1980. Shear zone geometry: a review. *J. Struct. Geol.* **2**, 83–99.

Rigassi, A. D. 1977a. Subdivision et datation de la molasse "d'eau douce inférieure" du plateau suisse. *Paleolab News* **1**, 1–36.
Rigassi, A. D. 1977b. Genèse tectonique du Jura: une nouvelle hypothèse. *Paleolab News* **2**, 1–27.
Royden, L. & Karner, G. D. in press. Flexure of the lithosphere beneath the Apennine and Carpathian foredeep basins. *Bull. Am. Ass. Petrol. Geol.*
Seed, H. B. & Wilson, S. D. 1967. The Turnagain Heights Landslide, Anchorage, Alaska. *J. Soil Mech. Found. Div., Proc. Am. Soc. civ. engng* **93(SM4)**, 325–353.
Siddans, A. W. B. 1984. Thrust tectonics. A mechanistic view from the West and Central Alps. *Tectonophysics* **104**, 257–281.
Terzaghi, M. 1923. *Soil Mechanics in Engineering Practice.* Wiley, New York.
Trümpy, R. 1980. An outline of the geology of Switzerland. (Part A). *Proc. 26th Int. Geol. Congr. Schweiz. geol. komm.*
Turcotte, D. & Schubert, G. 1982. *Applications of Continuum Physics to Geological Problems.* Wiley, New York.
Vialon, P., Bonnet, J. L., Mugnier, J. L. & Gamond, J. F. 1984. Modélisation des déformations d'une série stratifiée, par le déplacement horizontal d'un poinçon. Application au Jura. *Bull. Soc. géol. Fr.* **26**, 139–150.
Voight, B. 1973. The mechanics of retrogressive block-gliding, with emphasis on the evolution of the Turnagain-Heights Landslide, Anchorage, Alaska. In: *Gravity and Tectonics* (edited by Scholten, R. & De Jong, K.) Wiley, New York, 97–121.
Walcott, R. I. 1970. Isostatic response to loading of the crust in Canada. *Can. J. Earth Sci.* **7**, 716–727.
Weber, C. 1960. Etude de la partie septentrionale du faisceau de Syam (Jura). Thèse 3° Cycle. Paris University.
Winslow, M. A. 1981. Mechanisms for basement shortening in the Andean foreland belt of southern South America. In: *Thrust and Nappe Tectonics* (edited by McClay, K. & Price, N. J.). *Spec. Publs geol. Soc. Lond.* **9**, 513–528.

APPENDIX 1: SOURCES OF DATA

(1) Geologic maps edited by the *Bureau de Recherches Géologiques et Minières* (France), scale 1/50000, sheets: Champagnole, Lons-le-Saunier, Morez-Bois d'Amont, Poligny, Orgelet, Salins-les-bains.
(2) Geologic maps edited by the *Schweizerischen Geologischen Kommission.* Carte Geologique de la Suisse, Scale 1/500000. Atlas géologique de la Suisse, Scale 1/25000, sheet Vallée de Joux-le-Sentier, Marcheruz.
(3) Logs of drill holes, from N.W. to S.E.: 40 holes near the Bresse graben (Lienhardt 1962); Vaux-en-Poligny (notice accompanying the map-sheet Poligny); Valempoulières 1, 3, 102, 101; Thesy (Mugnier, 1984) Toilon (notice accompanying the map-sheet Champagnole); Risoux (notice accompanying the map-sheet Morez-Bois d'Amont); Chatel-Blanc; Morges, Jorat, Savigny, Pondeze, Pelerin, Vevey (Rigassi 1977a, and Matter & Homewood 1980). The logs of the French drill holes are preserved at the mining survey, Service Géologique Régional Rhône-Alpes, Lyon.
(4) Structural analysis from Plessmann (1972), Bonnet (1983), Mugnier (1984).
(5) Earthquakes focal mechanisms from Pavoni (1980), Dorel *et al.* 1983.